Biochemical Engineering Journal 159 (2020) 107602

Contents lists available at ScienceDirect

Biochemical Engineering Journal

journal homepage: www.elsevier.com/locate/bej

Regular article

Stimulation of cell growth and neurogenesis using protein-functionalized microfibrous scaffolds and fluid flow in bioreactors

Simon Grossemy, Peggy P.Y. Chan, Pauline M. Doran*

Faculty of Science, Engineering and Technology, Swinburne University of Technology, PO Box 218, Hawthorn, Melbourne, VIC 3122, Australia

HIGHLIGHTS

- PC12 cells were cultured in microfibrous scaffolds in bioreactors with continuous laminar fluid flow.
- Cells were subjected to hydrodynamic shear stresses between 2.7×10^{-5} and 4.6×10^{-3} Pa without damage.
- The integrity of protein-functionalized scaffold fibers was maintained under flow.
- Cell growth and neural differentiation were enhanced by fluid flow relative to static conditions.
- Neural differentiation was greater in scaffold cultures than in surface monolayers.

ARTICLE INFO

Keywords:
Bioreactor
Hydrodynamic shear stress
Microfibrous scaffolds
Neurogenesis

ABSTRACT

Microfibrous viscose-rayon scaffolds functionalized with poly-L-lysine and laminin were used to culture pheochromocytoma (PC12) cells in recirculation bioreactors under bulk laminar flow conditions. To determine the effects of continuous forced convective flow on cell viability, growth, and neurogenesis, the cultures were exposed to fluid-induced shear stresses of magnitude 2.7×10^{-5} to 4.6×10^{-3} Pa for up to 12 days. The results were compared with those obtained using static scaffold and static monolayer (2D) control cultures. Cell growth rates were 1.5- to 1.8-fold greater in the bioreactor scaffold cultures relative to the controls without flow. After treatment of the cells with nerve growth factor, development and extension of neurite networks and expression of several neural differentiation markers including β3-tubulin, shootin1, and EphA2 were also substantially enhanced in the presence of fluid convection. In the control cultures without fluid flow, cell growth and differentiation were greater in the static scaffold cultures than in the static 2D monolayers. This work demonstrates the significant beneficial effects of features of the physical culture environment, such as hydrodynamic conditions and cell attachment surface geometry, in regulating culture performance. Flow devices capable of supporting long-term cell culture while delivering controlled levels of hydrodynamic shear are a valuable practical tool for promoting nerve tissue development and regeneration *in vitro*.

1. Introduction

Acute trauma and degenerative diseases affecting the nervous system present major challenges in clinical medicine. Despite advances in surgical techniques, current treatments remain largely inadequate. The limited capacity of adult nerves for self-repair contributes to these difficulties. Inflammation-driven pathogenic responses in damaged brain and spinal cord tissue severely inhibit healing, and patients who undergo surgery for peripheral nerve repair often do not regain full motor or sensory function [1,2]. As a result, nerve injury and disease often lead to life-long disabilities, including paralysis, cognitive impairment, and sensory loss. New therapies are required to ease the morbidity, dysfunction, and economic cost associated with these conditions.

Nerve tissue engineering using biomaterial-supported cell culture systems holds significant promise as a therapeutic approach for nerve reconstruction and repair (reviewed in [3,4]). Crucial for the success of tissue engineering is the ability to closely manipulate environmental conditions to allow precise control of cell growth and differentiation. To date, most attention has been focused on the application of biochemical factors to influence neural cell behavior [5]. However, features of the biophysical environment, such as matrix material properties, architecture, and surface topography, can also provide transduction signals used by cells to direct neuronal lineage commitment and differentiation

* Corresponding author.
E-mail address: pdoran@swin.edu.au (P.M. Doran).

https://doi.org/10.1016/j.bej.2020.107602
Received 12 January 2020; Received in revised form 9 April 2020; Accepted 16 April 2020
Available online 21 April 2020
1369-703X/

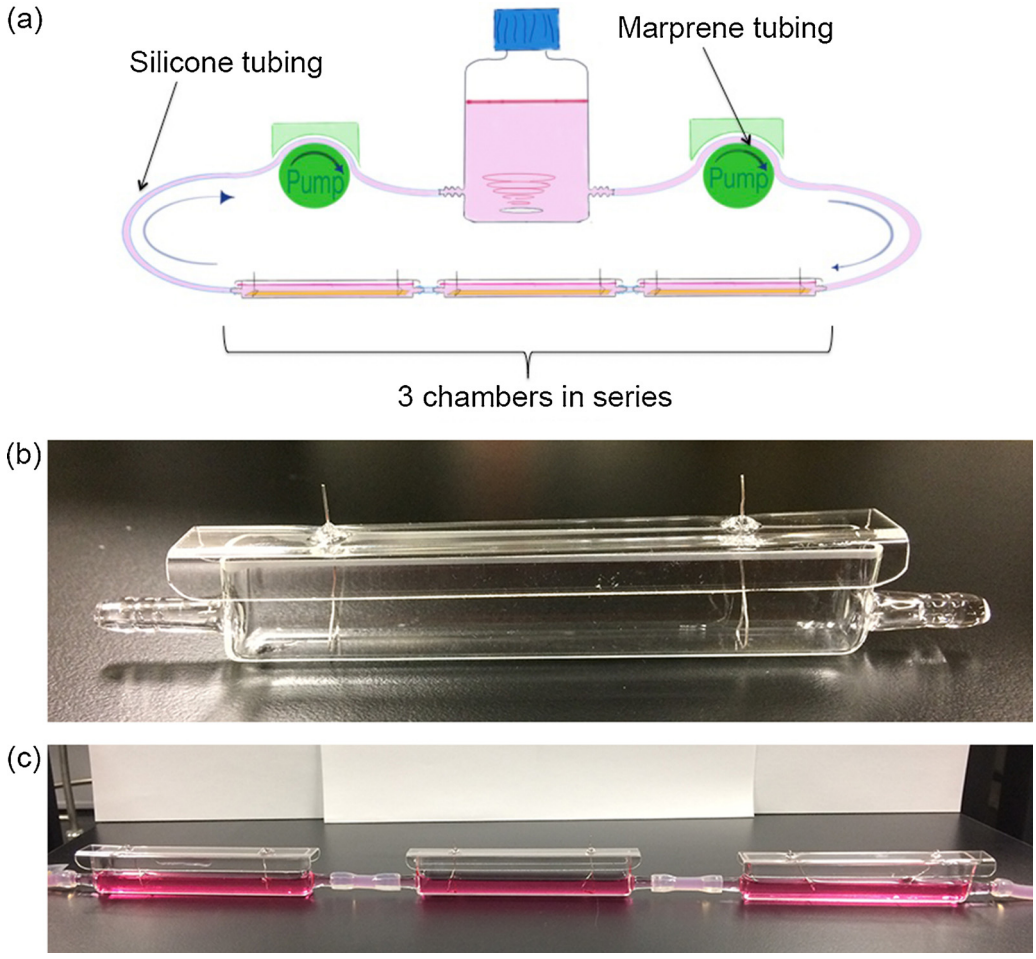

Fig. 1. Recirculation bioreactor system. (a) Schematic diagram of the bioreactor assembly comprising three bioreactor chambers in series connected to a medium bottle with pumps. (b) Photograph of a single glass bioreactor chamber with lid on. The wires shown were used to secure a scaffold to the base of the chamber. (c) Photograph of three bioreactor chambers containing culture medium connected in series using silicone tubing.

[6,7]. Culture of neural cells in porous three-dimensional (3D) scaffolds has been shown to reduce apoptosis and increase neurite differentiation compared with two-dimensional (2D) surface culture [8]. 3D culture systems mimic *in vivo* architectural conditions more closely than 2D cultures, thus providing a better matched environment for cell attachment and spatial organization and cell–cell interactions (reviewed in [9]). They also offer a closer representation of *in vivo* conditions for nutrient and oxygen distribution, as complex matrices constitute a mass transfer resistance for molecular diffusion and convection, resulting in the generation of concentration and charge gradients.

One aspect of the biophysical environment that has received relatively little attention in nerve tissue engineering is the provision of hydrodynamic forces or fluid flow during cell culture. Although studied for production of other tissues such as cartilage and bone (reviewed in [10]), application of convection bioreactors for neuronal differentiation of cells in 3D scaffolds is not widely reported [11,12]. Bioreactors generally allow better control of the chemical and physical conditions experienced by cells and may be designed to exert specific mechanical stimuli [13,14]. In the absence of fluid flow, high-density 3D cultures of neural cells risk becoming necrotic due to mass transfer limitations; however, in bioreactors providing perfusion of culture medium, cells within tissue constructs can be regularly replenished with nutrients and oxygen [15]. Dynamic fluid flow in bioreactors also subjects the cells to hydrodynamic forces that can function as a physical regulatory signal to trigger and promote cell growth and/or differentiation.

In this work, rat adrenal pheochromocytoma (PC12) cells were seeded into 3D microfibrous scaffolds and cultured under constant flow conditions in medium recirculation bioreactors. Immortalized PC12 cells are homogeneous and relatively easy to propagate and provide a well characterized model system for neurogenesis [16]. Nonwoven microfibrous viscose rayon, a cellulose-based material made from plant pulp, has been demonstrated previously to be an effective matrix for 3D culture of neuronal and neuroglial cells [17,18]. Responses of the cells to dynamic bioreactor culture were examined in terms of cell viability, growth, and neural differentiation and compared with cell properties observed in static 2D and static scaffold environments.

2. MATERIALS AND METHODS

2.1. Cells and Media

PC12 cells were maintained in Dulbecco's modified Eagle's medium containing 4.5 g L^{-1} glucose, 584 mg L^{-1} L-glutamine, and 3.7 g L^{-1} sodium bicarbonate (DMEM) with addition of 10% horse serum (Gibco: Life Technologies, Thermo Fisher, Melbourne, Australia), 5% fetal bovine serum (FBS) (Gibco: Life Technologies), and 1% penicillin-streptomycin antibiotic solution to give 100 U mL^{-1} penicillin and 100 µg mL^{-1} streptomycin. This medium is referred to as 'growth medium'. 'Differentiation medium' comprising DMEM with 1% horse serum, 1% penicillin-streptomycin solution, and 100 ng mL^{-1} nerve growth factor (NGF-7S) was used to induce neural differentiation. NGF was added fresh to the medium 1 h before its use.

2.2. Scaffolds and Cell Seeding

Scaffolds were prepared and seeded with PC12 cells as described previously [17]. Nonwoven microfibrous viscose rayon produced from plant cellulose fiber was obtained in sheet form as Azowipettes® (Synergy Health, Swindon, UK). The scaffold matrix exhibited an open fibrous structure with average fiber diameter 20 μm, pore sizes of 50–300 μm, and 66% porosity [18]. The scaffold thickness was 0.1 mm when the material was fully compressed for caliper measurement. Before seeding, the scaffolds were cut into 7 cm × 1 cm strips and functionalized using poly-L-lysine and laminin to promote cell adhesion. Poly-L-lysine was applied at a concentration of 100 μg mL^{-1} to provide a base coating on the fibers. The scaffolds were then washed three times in phosphate-buffered saline (PBS), exposed to 10 μg mL^{-1} of laminin, and washed a further three times. After 2 h of initial cell attachment at 37 °C, 95% humidity, and 5% CO_2, the scaffolds were incubated in growth medium for 2 days. For differentiation studies, the scaffolds were then incubated for a further 2 days in differentiation medium prior to the differentiation experiments.

2.3. Bioreactor

A recirculation bioreactor system was used to culture PC12 cells in microfibrous scaffolds under dynamic flow conditions (Fig. 1a). Each bioreactor assembly consisted of a medium reservoir connected to individual bioreactor chambers containing the scaffolds and cells. Two multichannel peristaltic pumps were used to recirculate medium through the chambers and control the flow conditions. Marprene tubing was used in the cassette pump heads. The medium reservoir was a 100-mL glass Schott bottle fitted with two tubing connector ports at the bottom. The bioreactor chambers (Fig. 1b) were custom-made from glass with length 9.3 cm, internal width 1.4 cm, and height 1.8 cm. Each chamber comprised two separate parts that fitted closely together for aseptic operation of the system: the bottom section of the chamber had hosing connectors at each end for medium flow and the top lid was removable. One 7 cm × 1 cm cell-seeded scaffold was placed flat along the bottom section of each bioreactor chamber and secured into position using two platinum wires fixed to the lid. Each complete bioreactor assembly comprised three bioreactor chambers in series (Fig. 1c) connected using silicone tubing to the pumps and medium reservoir (Fig. 1a).

The medium bottle, bioreactor chambers, and most of the tubing were placed inside an incubator at 37 °C, 95% humidity, and 5% CO_2. A custom-made port in the side of the incubator allowed tubing to pass through to the pumps that remained outside. Each bioreactor assembly was operated using 80 mL of medium. Liquid in the medium bottle was stirred constantly using a magnetic stirrer and the cap was loosened for gas exchange. During cell culture, the pumps were operated to give a volumetric flow rate of 0.51 mL min^{-1}, corresponding to a recirculation frequency of 9.2 day^{-1} for the entire 80 mL of medium in the system. The medium was changed partially every 2 days by removing 40 mL of spent medium and adding 40 mL of fresh medium. Cell growth and differentiation experiments were performed in triplicate using three independent recirculation bioreactor assemblies, each with three bioreactor chambers that could be harvested at different time points.

To determine the flow regime in the bioreactor, the Reynolds number *Re* was calculated as:

$$Re = \frac{\rho v D_h}{\mu} \tag{1}$$

where ρ is fluid density (1040 kg m^{-3}), v is superficial fluid velocity, D_h is hydraulic diameter, and μ is fluid dynamic viscosity (1.07×10^{-3} Pa s). The hydraulic diameter for a partially filled rectangular duct is given by the equation [19]:

$$D_h = \frac{4\times\text{cross-sectional area}}{\text{wetted perimeter}} = \frac{4hb}{2h + b} \tag{2}$$

where h is liquid height (0.85 cm) and b is width of the channel (1.4 cm). The superficial fluid velocity is defined as:

$$v = \frac{Q}{A} = \frac{Q}{hb} \tag{3}$$

where Q is volumetric flow rate (0.51 mL min^{-1}) and A is cross-sectional area for flow. Using Eqs (1)–(3), the Reynolds number for bioreactor operation was evaluated as 1.1, indicating that bulk flow in the bioreactors was laminar.

For fully developed, unidirectional laminar flow of a Newtonian fluid across a solid surface where the top of the fluid is open to the atmosphere, the wall shear stress τ_w is given by the equation [20]:

$$\tau_w = \frac{3\mu Q}{h^2 b} \tag{4}$$

Eq. (4) was used to estimate the laminar shear stress at the base of the bioreactor chambers. The average shear stress τ_{av} experienced by cells within the fibrous scaffolds was calculated as [21]:

$$\tau_{av} = \frac{3\pi}{8}\frac{\mu\,(0.1v)}{r_c}\left(1 + \frac{1}{\sigma}\right) \tag{5}$$

where r_c is cell radius (estimated from electron micrographs of seeded scaffolds as 3 μm [17]) and $0.1v$ is the free stream velocity at a depth of 0.1 mm above the base of the bioreactor chambers (estimated from the velocity profile for laminar flow in a rectangular duct [22]). The dimensionless permeability σ is given by the equation:

$$\sigma = \sqrt{\frac{k}{r_c^2}\left(1 + \frac{5}{2}(1-\varepsilon)\right)} \tag{6}$$

where k is permeability of the fibrous material and ε is its porosity or void volume fraction (0.66). The scaffold permeability k was estimated as 1.7×10^{-7} cm^2 using published correlations for low Reynolds number flow ($Re < 10$) through 3D arrays of randomly oriented rods or fibers [23,24] taking the diameter of the cell-coated fibers to be 20 μm plus an estimated 6-μm layer of attached cells = 26 μm. Eqs (5) and (6) were used to provide an order-of-magnitude estimate of the average shear stress experienced by cells within the fiber network of the scaffolds.

2.4. Cell Cultures

Scaffolds seeded with cells were cultured under constant flow conditions in the bioreactors either in growth medium for up to 12 days or in differentiation medium for 6 or 12 days. Static control cultures were also carried out. In one control, cells in scaffolds were cultured under static conditions in Petri dishes 9 cm in diameter × 1.4 cm high containing 12 mL of medium. For cell growth studies, growth medium in the Petri dishes was completely replaced every 2 days; for differentiation studies, 7 mL of spent medium was replaced with 7 mL of differentiation medium every 2 days. As a second control, static 2D monolayer cultures were carried out in 24-well plates coated with poly-L-lysine and laminin and containing 500 μL of medium per well. For cell growth studies, growth medium in the wells was completely replaced every 2 days; for differentiation studies, half medium replacement was carried out every 2 days using differentiation medium. Static control cultures were not performed in the bioreactors after preliminary observations indicated that nutrient and oxygen delivery was limited in the bioreactor system in the absence of liquid flow, and that culture performance was likely to be poor under these conditions.

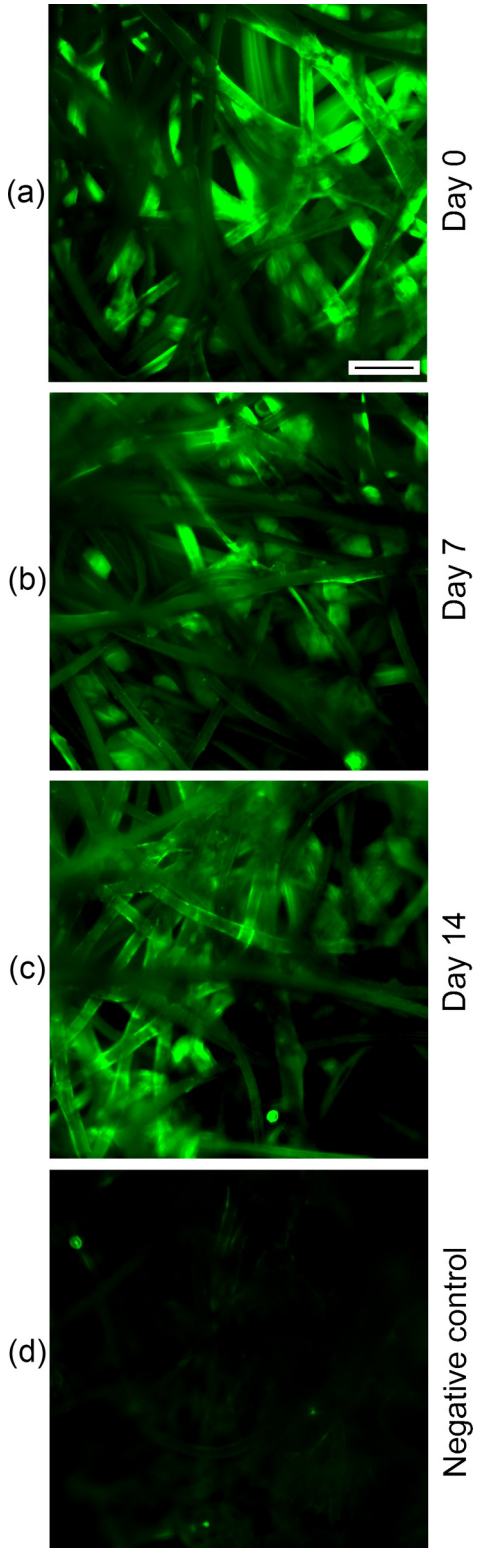

Fig. 2. Epifluorescence microscope images of scaffolds after immunochemical staining for laminin (green). The samples were coated with poly-L-lysine and laminin and placed in a bioreactor under constant flow conditions for (a) 0; (b) 7; and (c) 14 days. The negative control scaffolds (d) were treated with secondary antibody only. The scale bar in (a) represents 100 μm and applies to all images. The scaffolds showed good laminin coverage irrespective of their exposure to fluid flow.

2.5. Analyses

2.5.1. Scaffold Functionalization and Integrity

The functionalization and surface integrity of scaffolds coated with poly-L-lysine and laminin were assessed immunochemically after the scaffolds were subjected to constant bioreactor flow conditions in PBS at 37 °C for up to 14 days. Scaffolds removed from the bioreactor were incubated overnight at 4 °C with rabbit anti-laminin antibody (0.5 mg mL^{-1}: Sigma-Aldrich) diluted 1:60. The secondary antibody, donkey anti-rabbit Alexa Fluor® 488 (Invitrogen: Thermo Fisher) diluted 1:1000, was applied at room temperature in the dark for 2 h. The samples were observed using an epifluorescence microscope with excitation at 490 nm and emission at 525 nm. Three negative controls were tested: one with poly-L-lysine and laminin but without antibodies to check for scaffold autofluorescence, another with poly-L-lysine but no laminin to check the specificity of the primary antibody, and a third with poly-L-lysine and laminin treated with secondary antibody only.

2.5.2. Cell Number and Viability

Cell number was determined from DNA measurements using fluorometric Hoechst 33258 staining as described previously [17]. A cellular DNA content of 13.2 pg was measured for the PC12 cells and used to convert DNA quantity to cell number. Cell viability after 5 days of culture in growth medium was measured by flow cytometry. The cells were stained using a calcein AM/ethidium homodimer-1 live/dead staining kit and examined as described previously [17] using an Attune NxT flow cytometer with excitation at 488 nm and emission wavelengths of 530 nm and 695 nm.

2.5.3. PCR and Immunocytochemistry

Cells were examined after 6 and 12 days of culture in differentiation medium. Gene expression levels were measured quantitatively using real-time reverse transcription polymerase chain reaction (RT-PCR) as described previously [17]. The markers of neural differentiation examined by RT-PCR were nestin, β3-tubulin, shootin1, and ephrin type-A receptor 2 (EphA2). Ribosomal protein L19 (RPL19) was used as the housekeeping gene. Cells were subjected to immunocytochemical analysis *in situ* using antibodies against β3-tubulin and microtubule associated protein 2 (MAP2) as described previously [17]. Nuclei were stained using 4′,6-diamidino-2-phenylindole (DAPI). Negative controls were incubated with secondary antibody only. The immunolabeled samples were viewed using an epifluorescence microscope and confocal laser-scanning microscope with excitation/emission wavelengths of 405/450 nm for DAPI, 488/520 nm for β3-tubulin, and 561/595 nm for MAP2.

2.5.4. Statistics

Samples were harvested from triplicate cultures. Data from replicate cultures are presented as averages ± standard errors. Groups of data were compared using one-way analysis of variance (ANOVA) in conjunction with Tukey's test at $p < 0.05$ and $p < 0.01$ levels of significance.

3. Results

3.1. Bioreactor Hydrodynamic Conditions

For a medium recirculation rate of 0.51 mL min^{-1}, the superficial liquid velocity in the bioreactor chambers was 4.3 mm min^{-1}. The hydrodynamic shear stress τ_w was estimated using Eq. (4) as 2.7×10^{-5} Pa (2.7×10^{-5} N m^{-2} or 2.7×10^{-4} dyn cm^{-2}). This result reflects the shear characteristics of ideal one-dimensional laminar flow and approximates the wall shear stress exerted on cells at the base of the bioreactor chambers. Cells within the scaffolds experienced a different set of shear conditions due to interstitial flow of fluid within the scaffold pores. Using Eqs (5) and (6), the average shear stress τ_{av} experienced by cells

attached to the scaffold fibers was estimated as 4.6×10^{-3} Pa. Taken together, these values provide a rough indication of the range of fluid shear stresses generated in the bioreactors and experienced by the cells.

3.2. Scaffold Functionalization and Surface Integrity

To promote cell attachment, the scaffolds were coated with poly-L-lysine and laminin. The stability of this protein coating and integrity of the scaffold surface under bioreactor flow conditions were assessed using laminin immunostaining (Fig. 2). All three negative controls showed no or very little fluorescence, confirming that the observed green fluorescence was due only to the presence of laminin on the fibers. The epifluorescence images show some shadowing of the fibers, reflecting the 3D nature of the microfibrous scaffolds. There was no observable reduction in laminin fluorescence intensity with time under constant flow conditions, demonstrating that the protein coating on the scaffolds was resistant to the hydrodynamic environment in the bioreactor for up to 14 days.

3.3. Cell Viability and Growth

Results for the viability of attached cells in static 2D, static scaffold, and bioreactor scaffold cultures in growth medium are shown in Fig. 3. All cultures exhibited high cell viability levels of 89–94%. Statistically, cell viability was slightly higher in the static 2D and bioreactor scaffold cultures than in the static scaffold cultures ($p < 0.05$).

Time-course data for cell growth are shown in Fig. 4. Total numbers of attached cells per well or per scaffold are plotted for the different culture systems. The static scaffold and bioreactor scaffold cultures were initiated using the same number of cells (Fig. 4b); the lower initial cell number in the static 2D cultures (Fig. 4a) is consistent with the much smaller volume of medium in this system. The different geometries of the 2D and 3D scaffold cultures meant that no single measure of cell density, whether total number of cells, cells per mL of medium, cells cm^{-2}, or cells cm^{-3} of scaffold, was a practical option for providing equivalent starting conditions for all three cultures. Instead, the experiments were carried out using initial cell densities typical for each respective culture system. Attached cells in all cultures exhibited exponential growth. The maximum cell number reached after 6 days of bioreactor scaffold culture was significantly higher ($p < 0.01$) than the maximum achieved in the static scaffold cultures after 8 days (Fig. 4b).

During exponential growth, the cell specific growth rate is constant and independent of cell number. Accordingly, this parameter allows growth rates to be compared between systems with different cell densities. As shown in Fig. 5, specific growth rates in the bioreactor scaffold cultures were 1.8-fold greater than in the static 2D controls ($p < 0.01$) and 1.5-fold greater than in the static scaffold cultures ($p < 0.01$). Comparing the two static controls, growth rates in the scaffold cultures were 1.2-fold greater than in the 2D system ($p < 0.05$). Cell doubling

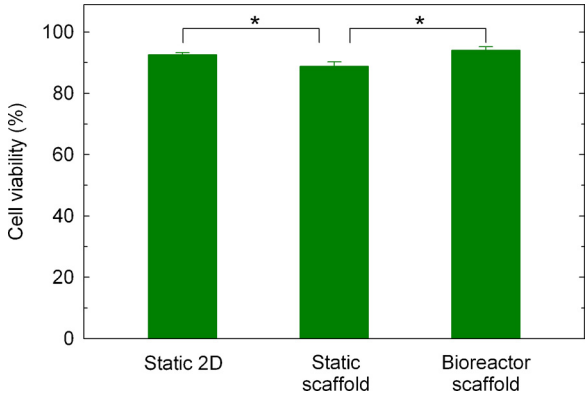

Fig. 3. Cell viability in static 2D, static scaffold, and bioreactor scaffold cultures after 5 days in growth medium. The error bars represent standard errors from triplicate cultures. Significant differences at the $p < 0.05$ level are indicated *.

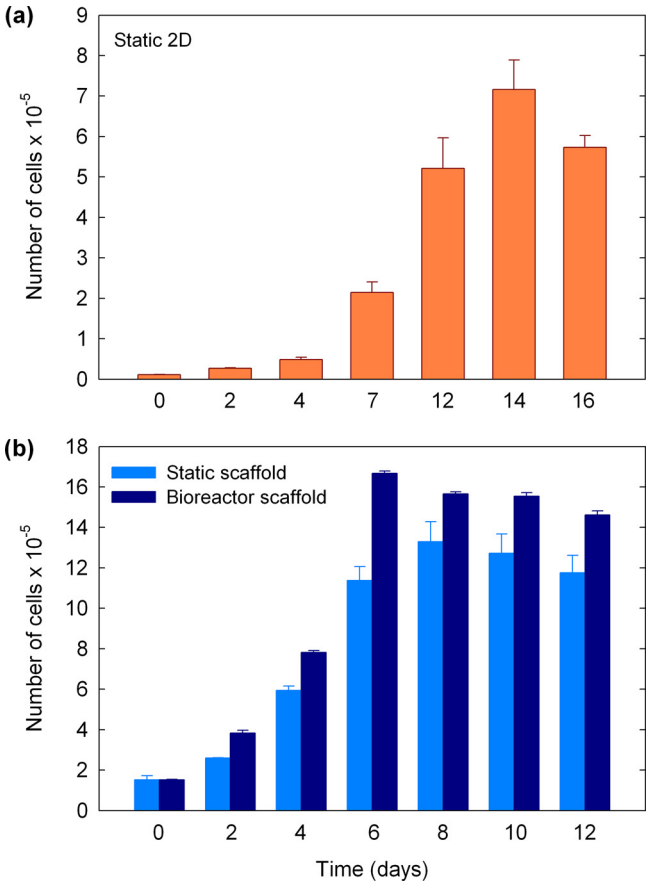

Fig. 4. Time-course results for growth of attached cells in (a) static 2D; and (b) static scaffold and bioreactor scaffold cultures. The number of attached cells per well in the static 2D cultures and the number of attached cells per scaffold in the static scaffold and bioreactor scaffold cultures are plotted. The error bars represent standard errors from triplicate cultures. All cultures exhibited exponential growth kinetics before reaching stationary phase.

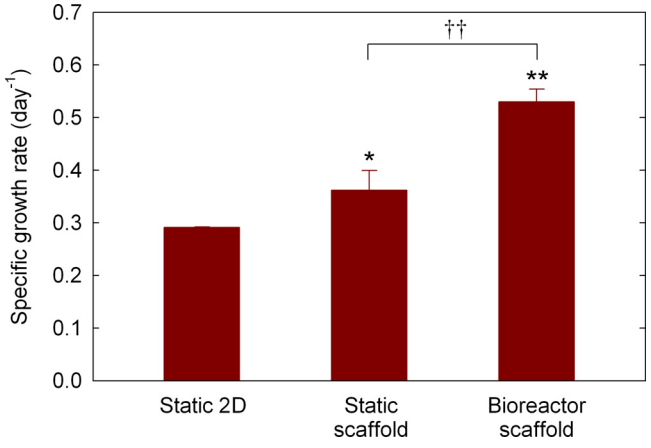

Fig. 5. Cell specific growth rates during the exponential growth phase for static 2D, static scaffold, and bioreactor scaffold cultures. During exponential growth, the cell specific growth rate is constant and independent of cell number. The error bars represent standard errors from triplicate cultures. Significant differences relative to the static 2D cultures at the $p < 0.05$ and $p < 0.01$ levels are indicated * and **, respectively. Significant difference between the static scaffold and bioreactor scaffold cultures at the $p < 0.01$ level is indicated ††.

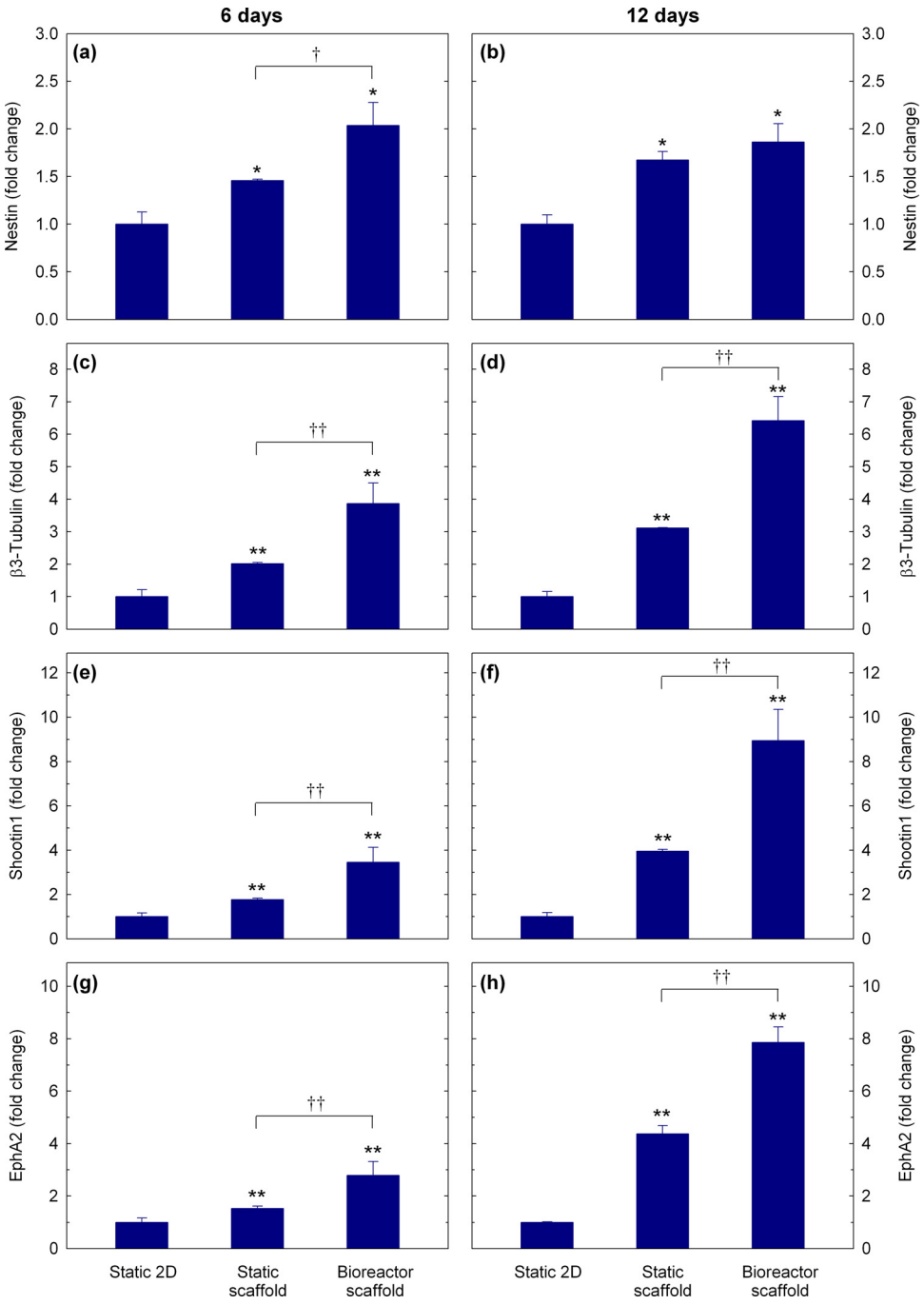

Fig. 6. Gene expression levels in static 2D, static scaffold, and bioreactor scaffold cultures. The cells were cultured in differentiation medium for (a), (c), (e), and (g) 6 days, or (b), (d), (f), and (h) 12 days. The differentiation markers tested were nestin, β3-tubulin, shootin1, and EphA2. For each marker and culture duration, the results are expressed relative to the corresponding transcript levels for static 2D cultures. The error bars represent standard errors from triplicate cultures. Significant differences relative to the static 2D cultures at the $p < 0.05$ and $p < 0.01$ levels are indicated * and **, respectively. Significant differences between the static scaffold and bioreactor scaffold cultures at the $p < 0.05$ and $p < 0.01$ levels are indicated † and ††, respectively.

times corresponding to these specific growth rates were 2.4, 1.9, and 1.3 days for the static 2D, static scaffold, and bioreactor scaffold cultures, respectively. Overall, these results indicate that dynamic bioreactor scaffold culture supported significantly faster cell growth than either the 2D or scaffold cultures under static conditions.

3.4. Neural Differentiation

To induce neural differentiation, cells in static 2D, static scaffold, and bioreactor scaffold systems were cultured for 6 and 12 days in differentiation medium containing NGF. Results from quantitative RT-PCR analysis of gene expression under these conditions are shown in Fig. 6. For each differentiation marker and culture duration, transcript levels are expressed relative to the results for the static 2D cultures.

Nestin is associated with the early stages of embryonic nerve tissue development and is downregulated as neural differentiation proceeds [25]. After 6 days of culture (Fig. 6a), its expression in the bioreactors was 2.0-fold greater than in the static 2D controls ($p < 0.05$) and 1.4-fold greater than in the static scaffold cultures ($p < 0.05$). After 12 days (Fig. 6b), nestin expression in the bioreactor cultures was 1.9-fold greater than in the static 2D controls ($p < 0.05$). Increased nestin expression in the static scaffold cultures relative to the static 2D controls was also significant after 6 and 12 days ($p < 0.05$) (Fig. 6a, 6b).

β3-Tubulin is a structural component of cytoskeletal microtubules and plays a crucial role in neurite outgrowth and neuronal morphogenesis [26]. Its expression is a marker of neuronal lineage commitment and differentiation. β3-Tubulin transcript levels after 6 days of bioreactor culture (Fig. 6c) were 3.9-fold greater than in the static 2D controls ($p < 0.01$) and 1.9-fold greater than in the static scaffold cultures ($p < 0.01$). After 12 days (Fig. 6d), β3-tubulin expression in

the bioreactor cultures was 6.4-fold greater than in the static 2D controls ($p < 0.01$) and 2.1-fold greater than in the static scaffold cultures ($p < 0.01$). β3-Tubulin expression was also higher in the static scaffold cultures than in the static 2D controls by a factor of 2.0 ($p < 0.01$) after 6 days and 3.1 ($p < 0.01$) after 12 days (Fig. 6c, 6d).

The effects of bioreactor culture on expression of shootin1 and EphA2 were similar to those observed for β3-tubulin. Shootin1 is involved in neuronal polarization and axon induction in early-stage neuritogenesis [27]; EphA2 regulates neural lineage commitment and neural cell adhesion, extension, and spreading [28,29]. In the bioreactors after 6 days of culture, shootin1 expression was enhanced 3.5-fold relative to the static 2D controls ($p < 0.01$) and 1.9-fold relative to the static scaffold cultures ($p < 0.01$) (Fig. 6e), while EphA2 expression was enhanced 2.8-fold relative to the static 2D controls ($p < 0.01$) and 1.8-fold relative to the static scaffold cultures ($p < 0.01$) (Fig. 6g). After 12 days of culture, shootin1 expression was 8.9-fold greater in the bioreactor cultures than in the static 2D controls ($p < 0.01$) and 2.3-fold greater in the bioreactors relative to the static scaffold cultures ($p < 0.01$) (Fig. 6f), while EphA2 expression was enhanced 7.9-fold relative to the static 2D controls ($p < 0.01$) and 1.8-fold relative to the static scaffold cultures ($p < 0.01$) (Fig. 6h). As observed for β3-tubulin, increased expression of shootin1 and EphA2 in the static scaffold cultures relative to the static 2D controls was also significant after 6 and 12 days ($p < 0.01$) (Fig. 6e–6 h).

Results from immunocytochemical staining for β3-tubulin and MAP2 are shown in Figs. 7–9. Additional images from these analyses are provided as Supplementary Material. Cells in static 2D (Fig. 7), static scaffold (Fig. 8), and bioreactor scaffold (Fig. 9) cultures were observed after 6 and 12 days of culture in differentiation medium. Neurite extension indicating cell morphological differentiation occurred in all treatment groups. Quantification of neurite number and length could not be reliably performed using these images because of the fibrous 3D structure of the scaffolds and associated masking and foreshortening effects. However, particularly in the scaffold cultures (Figs. 8 and 9), neurite processes after 12 days were longer and more abundant than at 6 days, indicating more advanced neurogenesis at 12 days. The images in Fig. 9 for the bioreactor scaffold cultures show no evidence of cell alignment within the scaffolds in response to the constant unidirectional flow of medium in the bioreactors. Neurite extension occurred in all directions in both the static and bioreactor scaffold cultures (Figs. 8 and 9), likely reflecting the random orientation of the scaffold fibers.

Immunostaining images for the bioreactor scaffold cultures, especially after 12 days (Fig. 9b, 9c), show the development of denser neurite networks with longer cellular processes than those found in the static 2D (Fig. 7) and static scaffold (Fig. 8) cultures. This confirms the results of the PCR analysis (Fig. 6) indicating enhanced neural differentiation in the bioreactors compared with both forms of static cell culture. The relatively limited development of neurite extensions in the static 2D cultures (Fig. 7) compared with the static scaffold cultures (Fig. 8) is also consistent with the PCR data for these systems (Fig. 6), demonstrating the beneficial effects of using microfibrous scaffolds for neural differentiation compared with 2D monolayer culture.

Overall, the PCR and immunocytochemistry results show that neural differentiation reached a more advanced state in the bioreactors than under static culture conditions. Furthermore, neural differentiation under static conditions was greater in the scaffolds than in the 2D monolayer cultures.

4. Discussion

Scaffold culture of PC12 cells in recirculation bioreactors under bulk laminar flow conditions produced substantial benefits compared with static cultures. Exposure of the cells to continuous flow of medium greatly improved cell proliferation rates (Fig. 5) as well as several quantitative and qualitative indicators of neural differentiation (Figs. 6–9). The scaffold-based culture system and recirculation device examined in this study support long-term cell and tissue development in a dynamic flow environment and offer significant practical advantages for promoting neural differentiation and regeneration *in vitro*.

Attached cells cultured in the presence of fluid flow experience hydrodynamic shear forces that develop in fluids as a result of local changes in fluid velocity. When fluid flows across a solid surface or through a porous matrix, such as in the bioreactor chambers and microfibrous scaffolds used in this work, shear forces are induced at and near the interface between the fluid and solid material. Cells attached to those surfaces are exposed to the generated shear stresses. Using two different theoretical approaches, the magnitude of the hydrodynamic shear stress applied to cells in this study was estimated as 2.7×10^{-5} to 4.6×10^{-3} Pa. Both sets of model equations can be considered to provide approximate values that, taken together, define a plausible order-of-magnitude range for the fluid shear stresses experienced by the cells. The average shear stress for flow within the scaffolds (4.6×10^{-3} Pa) is considerably greater than the wall shear stress calculated for laminar flow outside the scaffolds (2.7×10^{-5} Pa). This reflects the amplification of shear forces in the scaffolds due to spatial restriction of the interstitial flow paths resulting in relatively high local linear velocities in the vicinity of the cells. Estimating the hydrodynamic properties of interstitial flow within the pores of 3D scaffolds is much more challenging than for 2D systems because of the complex architecture of the scaffold material and heterogeneous nature of the internal fluid velocities [30,31]. The shear stress estimated here for the scaffolds is derived from a continuum model that averages the resistance to flow offered by the fibrous matrix across the entire flow domain.

As well as directly sensing the hydrodynamic shear forces induced by fluid flow, attached cells in flow systems are also subject to various indirect drag and tethering forces associated with matrix adhesion [32,33]. Matrix tension arising from changes in the scaffold itself, e.g. compression, fiber realignment, or erosion, in response to the forces generated by flow may also be transmitted to the cells [31,34]. Such indirect effects of fluid convection depend on characteristics of the scaffold matrix including its architecture, deformability, and cell adhesion properties.

The combined forces associated with fluid flow are known to trigger biological mechano-transduction processes in cells that convert exogenous mechanical stimuli into intracellular biochemical activity [32,35]. A wide range of beneficial responses in terms of flow-induced gene expression, cell proliferation, lineage commitment, and differentiation has been observed after exposure of different cell types to fluid shear [36]. Supply of nutrients and oxygen to cells is also improved by flow, as convective currents can overcome any mass transfer deficiencies in the culture system [15]. Distinguishing between these two different hydrodynamic mechanisms for enhancing cell performance, i.e. direct mechano-stimulation of the cells and improved mass transfer, is often difficult experimentally [37]. Because exposure to shear forces can cause lytic or sublytic cell damage, the magnitude, timing, and manner of application of any mechanical stimulus must be closely regulated. The estimated fluid shear levels in the bioreactors in this work (2.7×10^{-5} to 4.6×10^{-3} Pa) are low relative to those generally regarded as damaging to cultured mammalian cells (1–10 Pa [38]) or those used to elicit flow-induced shear trauma in cultured neurons (1.0–4.5 Pa [39,40]). We can conclude therefore that the average hydrodynamic shear forces generated in the bioreactors were well below levels capable of causing cell damage.

Relatively low fluid shear stresses similar to those examined here are characteristic of rotating wall vessels operated under microgravity conditions and some microfluidic perfusion systems (e.g. [37,41,42]. However, in most studies of hydrodynamic effects on cells, other types of flow apparatus are used to deliver significantly higher levels of shear typically in the range of 0.1–3 Pa [13,43–45]. For PC12 cells on 2D surfaces, whereas intermittent application of 0.25 Pa of fluid shear was found to increase the length of neurites relative to untreated controls,

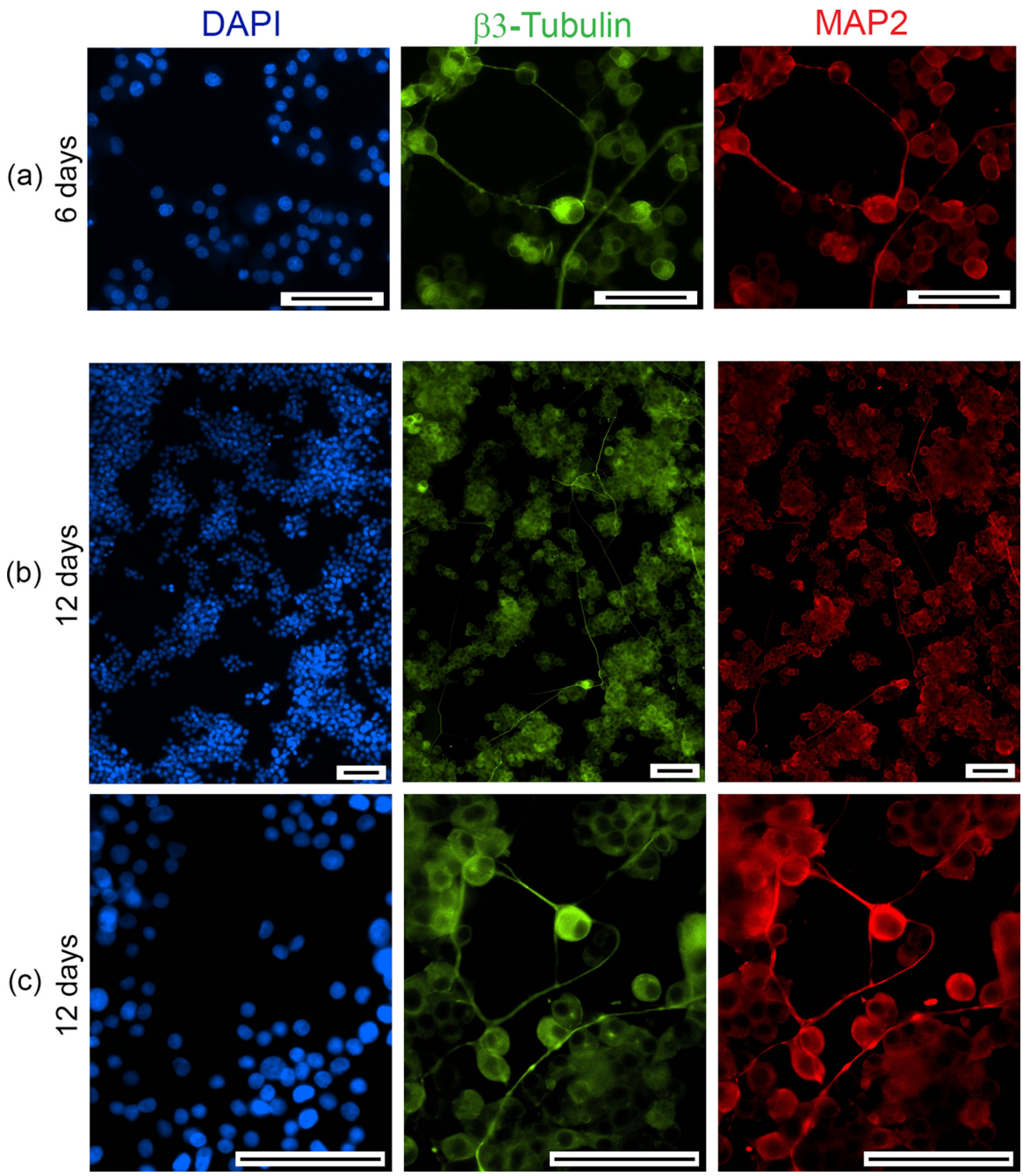

Fig. 7. Epifluorescence microscope images of cells in static 2D cultures after staining for DAPI (blue), β3-tubulin (green) and MAP2 (red). The cells were cultured in differentiation medium for (a) 6 days; and (b), (c) 12 days. All scale bars represent 100 μm.

continuous application of the same stimulus for 48 h resulted in cell detachment [13]. In contrast and most likely as a consequence of the lower shear levels imposed, no significant problems with growth of attached cells (Figs. 4 and 5), cell viability (Fig. 3), or neurite development (Fig. 9) were observed in the bioreactor cultures in the current work, even though the cells were subjected to continuous fluid flow over an extended period of 12 days. The laminin surface coating on the scaffold fibers was also found to withstand the continuous flow conditions applied (Fig. 2).

In previous studies, particularly with osteogenic cells, oscillatory or reciprocal fluid flow has been applied to cultures at a frequency of 1 Hz to mimic the effects of ambulatory exercise [45,46]. However, the benefits compared with steady, unidirectional fluid flow are unclear, as a diverse range of outcomes has been reported using this form of flow stimulus (e.g. [47–49]). For this reason, and because neuronal differentiation involves the extension of very thin neurite processes that could be disrupted by rapid reversals in flow direction, fluctuating regimes of fluid flow were not implemented in the current work. Cell alignment in flow systems has been observed in previous studies with various cell types [12,13,50], often under the influence of micropatterned surface topography or aligned scaffold features. Neurite alignment was not observed in the present study (Fig. 9) even with application of unidirectional fluid flow, most likely because the cells were attached to a random arrangement of fibers within the scaffolds. Because flow-induced cell alignment requires laminar flow conditions, any development of small-scale local turbulence within the interstitial microenvironment of the scaffolds would also act to prevent uniform orientation of the cells [50].

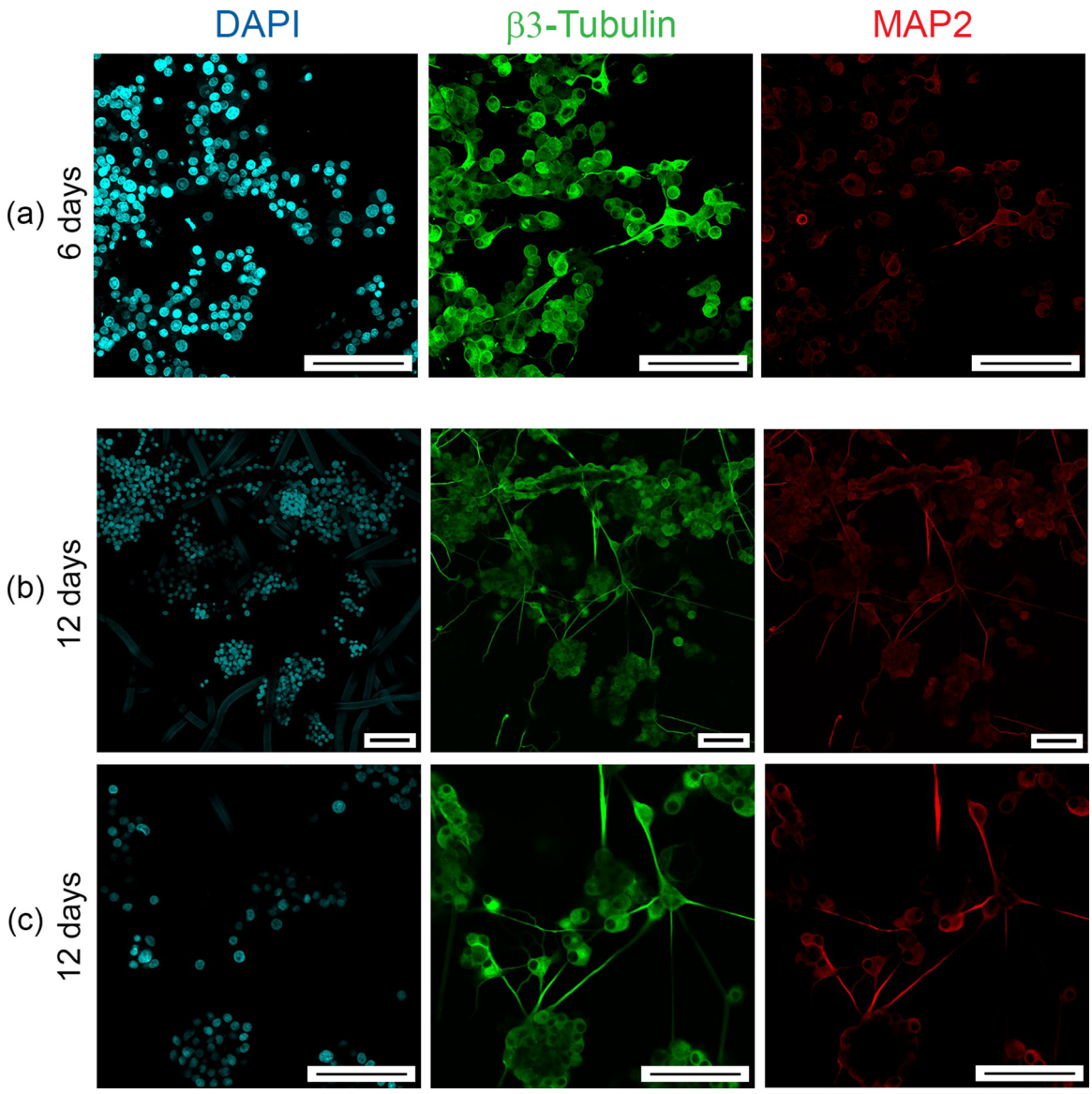

Fig. 8. Confocal microscope images of cells in static scaffold cultures after staining for DAPI (blue), β3-tubulin (green) and MAP2 (red). The cells were cultured in differentiation medium for (a) 6 days; and (b), (c) 12 days. All scale bars represent 100 μm. Images in (a) and (c) are reproduced from [17] by permission of Oxford University Press.

In the absence of fluid flow, cell growth rates (Fig. 5) and neural differentiation (Figs. 6–8) were enhanced by culturing cells in microfibrous scaffolds rather than as 2D monolayers. Cell attachment surfaces in both types of static culture were functionalized using poly-L-lysine and laminin. In previous studies, neural progenitor cells in 3D hydrogel scaffolds showed improved cell viability and β3-tubulin expression relative to 2D cultures [51], and neurite length was increased when PC12 cells were cultured in 3D fibrin scaffolds rather than in 2D [8]. Although delivery of nutrients and oxygen to cells can be impaired in static 3D scaffolds, comparison of results for the static 2D and static scaffold cultures in the present work (Figs. 3,5–8) provides no evidence for any significant detrimental effects in the scaffolds due to mass transfer limitations. This may be attributed to the very small thickness of the scaffolds and the open structure of the scaffold fibrous network.

5. Conclusions

Application of bioreactors for neuronal differentiation of cells in 3D scaffolds has received relatively little attention for nerve tissue engineering. In this study, cells in surface-functionalized microfibrous scaffolds were exposed to continuous fluid-induced shear stress for up to 12 days in recirculation bioreactors. Cell growth, expression of neural differentiation markers, and morphological development of neurites were all substantially improved in the bioreactor scaffold cultures compared with static 2D and static scaffold systems. These findings demonstrate that laminar flow devices delivering relatively low average levels of hydrodynamic shear over extended culture periods offer significant advantages for *in vitro* neural cell growth and development. In addition, in the absence of fluid flow, static 3D scaffold cultures were found to support faster cell growth and more advanced levels of neural differentiation than static 2D monolayers.

Declaration of Competing Interest

The authors declare that they have no known competing financial interests or personal relationships that could have appeared to influence the work reported in this paper.

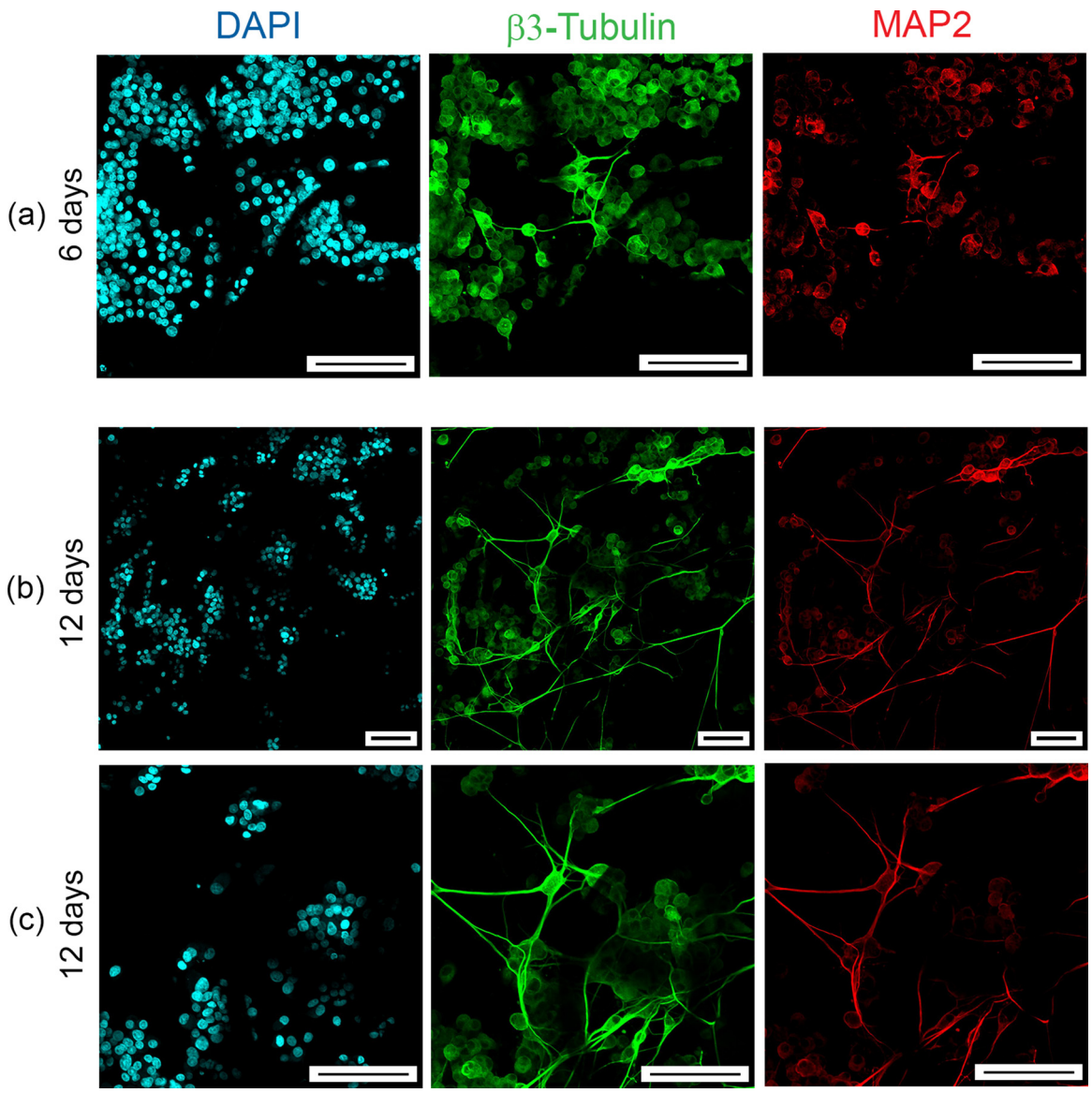

Fig. 9. Confocal microscope images of cells in bioreactor scaffold cultures after staining for DAPI (blue), β3-tubulin (green) and MAP2 (red). The cells were cultured in differentiation medium for (a) 6 days; and (b), (c) 12 days. All scale bars represent 100 μm. Complex neurite networks were developed in the bioreactor scaffold cultures, especially after 12 days.

CRediT authorship contribution statement

Simon Grossemy: Methodology, Investigation, Formal analysis, Writing - original draft, Writing - review & editing, Visualization. **Peggy P.Y. Chan:** Conceptualization, Writing - review & editing, Supervision, Funding acquisition. **Pauline M. Doran:** Conceptualization, Methodology, Writing - review & editing, Visualization, Supervision, Funding acquisition.

Acknowledgements

This work was funded by the Australian Research Council (ARC), grant number DP120102570. We thank Katharine Adcroft, Rebecca Alfred, and Shanti Krishnan for technical advice and assistance with the flow cytometry and PCR.

Appendix A. Supplementary data

Supplementary material related to this article can be found, in the online version, at doi:https://doi.org/10.1016/j.bej.2020.107602.

References

[1] D. Grinsell, C.P. Keating, Peripheral nerve reconstruction after injury: a review of clinical and experimental therapies, BioMed Res. Internat. 2014 (2014) 698256.
[2] B.S. Mietto, K. Mostacada, A.M.B. Martinez, Neurotrauma and inflammation: CNS and PNS responses, Mediators Inflamm. 2015 (2015) 251204.
[3] R. Boni, A. Ali, A. Shavandi, A.N. Clarkson, Current and novel polymeric biomaterials for neural tissue engineering, J. Biomed. Sci. 25 (2018) 90.
[4] S. Mobini, Y.H. Song, M.W. McCrary, C.E. Schmidt, Advances in ex vivo models and lab-on-a-chip devices for neural tissue engineering, Biomaterials 198 (2019) 146–166.
[5] M.E. Önger, B. Delibaş, A.P. Türkmen, E. Erener, B.Z. Altunkaynak, S. Kaplan, The role of growth factors in nerve regeneration, Drug Discov. Ther. 10 (2016) 285–291.
[6] S. Yao, X. Liu, X. Wang, A. Merolli, X. Chen, F. Cui, Directing neural stem cell fate with biomaterial parameters for injured brain regeneration, Prog. Nat. Sci.: Mater. Internat. 23 (2013) 103–112.
[7] J.M. Stukel, R.K. Willits, Mechanotransduction of neural cells through cell–substrate interactions, Tissue Eng. B 22 (2016) 173–182.
[8] S. Sadri, M. Khazaei, A. Ghanbari, M.R. Khazaei, P. Shah, Neuronal differentiation of PC12 and embryonic stem cells in two- and three-dimensional *in vitro* culture, Ind. J. Exp. Biol. 52 (2014) 305–311.
[9] B.M. Baker, C.S. Chen, Deconstructing the third dimension – how 3D culture microenvironments alter cellular cues, J. Cell Sci. 125 (2012) 3015–3024.
[10] A. Ravichandran, Y. Liu, S.-H. Teoh, Review: bioreactor design towards generation of relevant engineered tissues: focus on clinical translation, J. Tissue Eng. Regen.

Med. 12 (2018) e7–e22.
[11] H.J. Lin, T.J. O'Shaughnessy, J. Kelly, W. Ma, Neural stem cell differentiation in a cell–collagen–bioreactor culture system, Dev. Brain Res. 153 (2004) 163–173.
[12] S. Morelli, A. Piscioneri, S. Salerno, C.-C. Chen, C.H. Chew, L. Giorno, E. Drioli, L. De Bartolo, Microtube array membrane bioreactor promotes neuronal differentiation and orientation, Biofabrication 9 (2017) 025018.
[13] I.A. Kim, S.A. Park, Y.J. Kim, S.-H. Kim, H.J. Shin, Y.J. Lee, S.G. Kang, J.-W. Shin, Effects of mechanical stimuli and microfiber-based substrate on neurite outgrowth and guidance, J. Biosci. Bioeng. 101 (2006) 120–126.
[14] Q. Xu, F. Chen, Y. Wang, X. Li, J. He, Development of a miniaturized bioreactor for neural culture and axon stretch growth, Proc. 36th Ann. Internat. Conf. IEEE Engineering in Medicine and Biology Society (EMBC), Chicago USA, 26–30 August, 2014, pp. 1416–1419.
[15] D.K. Cullen, J. Vukasinovic, A. Glezer, M.C. LaPlaca, Microfluidic engineered high cell density three-dimensional neural cultures, J. Neural Eng. 4 (2007) 159–172.
[16] K. Fujita, P. Lazarovici, G. Guroff, Regulation of the differentiation of PC12 pheochromocytoma cells, Environ. Health Perspect. 80 (1989) 127–142.
[17] S. Grossemy, P.P.Y. Chan, P.M. Doran, Electrical stimulation of cell growth and neurogenesis using conductive and nonconductive microfibrous scaffolds, Integr. Biol. 11 (2019) 264–279.
[18] T. Sun, D. Norton, N. Vickers, S.L. McArthur, S. MacNeil, A.J. Ryan, J.W. Haycock, Development of a bioreactor for evaluating novel nerve conduits, Biotechnol. Bioeng. 99 (2008) 1250–1260.
[19] D.F. Elger, Engineering Fluid Mechanics, 11th ed., Wiley, Hoboken, 2016 pp. 335, 485.
[20] J.D. Humphrey, S.L. O'Rourke, An Introduction to Biomechanics, Springer, New York, 2015 p. 465.
[21] J.A. Pedersen, F. Boschetti, M.A. Swartz, Effects of extracellular fiber architecture on cell membrane shear stress in a 3D fibrous matrix, J. Biomech. 40 (2007) 1484–1492.
[22] R.K. Shah, A.L. London, Laminar Flow Forced Convection in Ducts, Academic Press, New York, 1978, pp. 197–198.
[23] G.W. Jackson, D.F. James, The permeability of fibrous porous media, Can. J. Chem. Eng. 64 (1986) 364–374.
[24] A. Koponen, D. Kandhai, E. Hellén, M. Alava, A. Hoekstra, M. Kataja, K. Niskanen, P. Sloot, J. Timonen, Permeability of three-dimensional random fiber webs, Phys. Rev. Lett. 80 (1998) 716–719.
[25] A.V. Gilyarov, Nestin in central nervous system cells, Neurosci. Behav. Physiol. 38 (2008) 165–169.
[26] C.D. Katsetos, M.M. Herman, S.J. Mörk, Class III β-tubulin in human development and cancer, Cell Motil. Cytoskeleton 55 (2003) 77–96.
[27] V. Ergin, M. Erdogan, A. Menevse, Regulation of shootin1 gene expression involves NGF-induced alternative splicing during neuronal differentiation of PC12 cells, Sci. Rep. 5 (2015) 17931.
[28] M. Aoki, T. Yamashita, M. Tohyama, EphA receptors direct the differentiation of mammalian neural precursor cells through a mitogen-activated protein kinase-dependent pathway, J. Biol. Chem. 279 (2004) 32643–32650.
[29] D.G. Wilkinson, Multiple roles of Eph receptors and ephrins in neural development, Nature Rev. Neurosci. 2 (2001) 155–164.
[30] B. Porter, R. Zauel, H. Stockman, R. Guldberg, D. Fyhrie, 3-D computational modeling of media flow through scaffolds in a perfusion bioreactor, J. Biomech. 38 (2005) 543–549.
[31] J.A. Pedersen, S. Lichter, M.A. Swartz, Cells in 3D matrices under interstitial flow: effects of extracellular matrix alignment on cell shear stress and drag forces, J. Biomech. 43 (2010) 900–905.
[32] W.J. Polacheck, A.E. German, A. Mammoto, D.E. Ingber, R.D. Kamm, Mechanotransduction of fluid stresses governs 3D cell migration, Proc. Natl Acad. Sci. U.S.A. 111 (2014) 2447–2452.
[33] L. You, S.C. Cowin, M.B. Schaffler, S. Weinbaum, A model for strain amplification in the actin cytoskeleton of osteocytes due to fluid drag on pericellular matrix, J. Biomech. 34 (2001) 1375–1386.
[34] J.J. Mack, K. Youssef, O.D.V. Noel, M.P. Lake, A. Wu, M.L. Iruela-Arispe, L.-S. Bouchard, Real-time maps of fluid flow fields in porous biomaterials, Biomaterials 34 (2013) 1980–1986.
[35] A. Mammoto, T. Mammoto, D.E. Ingber, Mechanosensitive mechanisms in transcriptional regulation, J. Cell Sci. 125 (2012) 3061–3073.
[36] L. Adamo, G. García-Cardeña, Directed stem cell differentiation by fluid mechanical forces, Antioxid. Redox Signal. 15 (2011) 1463–1473.
[37] K. Blagovic, L.Y. Kim, J. Voldman, Microfluidic perfusion for regulating diffusible signaling in stem cells, PLoS ONE 6 (8) (2011) e22892.
[38] R.S. Cherry, Animal cells in turbulent fluids: details of the physical stimulus and the biological response, Biotechnol. Adv. 11 (1993) 279–299.
[39] D. Kilinc, G. Gallo, K.A. Barbee, Mechanically-induced membrane poration causes axonal beading and localized cytoskeletal damage, Exp. Neurol. 212 (2008) 422–430.
[40] M. Liu, W. Song, P. Li, Y. Huang, X. Gong, G. Zhou, X. Jia, L. Zheng, Y. Fan, Galanin protects against nerve injury after shear stress in primary cultured rat cortical neurons, PLoS ONE 8 (5) (2013) e63473.
[41] M.N. Cinbiz, R.S. Tığlı, I.G. Beşkardeş, M. Gümüşderelioğlu, Ü. Çolak, Computational fluid dynamics modeling of momentum transport in rotating wall perfused bioreactor for cartilage tissue engineering, J. Biotechnol. 150 (2010) 389–395.
[42] W. Yu, H. Qu, G. Hu, Q. Zhang, K. Song, H. Guan, T. Liu, J. Qin, A microfluidic-based multi-shear device for investigating the effects of low fluid-induced stresses on osteoblasts, PLoS ONE 9 (2) (2014) e89966.
[43] R. Gupta, L. Truong, D. Bear, D. Chafik, E. Modafferi, C.T. Hung, Shear stress alters the expression of myelin-associated glycoprotein (MAG) and myelin basic protein (MBP) in Schwann cells, J. Orthop. Res. 23 (2005) 1232–1239.
[44] K.J. Jeon, S.H. Park, J.W. Shin, Y.G. Kang, J.-S. Hyun, M.J. Oh, S.Y. Kim, J.-W. Shin, Combined effects of flow-induced shear stress and micropatterned surface morphology on neuronal differentiation of human mesenchymal stem cells, J. Biosci. Bioeng. 117 (2014) 242–247.
[45] R.J. McCoy, F.J. O'Brien, Influence of shear stress in perfusion bioreactor cultures for the development of three-dimensional bone tissue constructs: a review, Tissue Eng. B 16 (2010) 587–601.
[46] E. Stavenschi, M.-N. Labour, D.A. Hoey, Oscillatory fluid flow induces the osteogenic lineage commitment of mesenchymal stem cells: the effect of shear stress magnitude, frequency, and duration, J. Biomech. 55 (2017) 99–106.
[47] C.R. Jacobs, C.E. Yellowley, B.R. Davis, Z. Zhou, J.M. Cimbala, H.J. Donahue, Differential effect of steady versus oscillating flow on bone cells, J. Biomech. 31 (1998) 969–976.
[48] S.M. Ponik, J.W. Triplett, F.M. Pavalko, Osteoblasts and osteocytes respond differently to oscillatory and unidirectional fluid flow profiles, J. Cell. Biochem. 100 (2007) 794–807.
[49] B. Roy, T. Das, D. Mishra, T.K. Maiti, S. Chakraborty, Oscillatory shear stress induced calcium flickers in osteoblast cells, Integr. Biol. 6 (2014) 289–299.
[50] Y. Li, G. Huang, X. Zhang, L. Wang, Y. Du, T.J. Lu, F. Xu, Engineering cell alignment *in vitro*, Biotechnol. Adv. 32 (2014) 347–365.
[51] S. Ortinau, J. Schmich, S. Block, A. Liedmann, L. Jonas, D.G. Weiss, C.A. Helm, A. Rolfs, M.J. Frech, Effect of 3D-scaffold formation on differentiation and survival in human neural progenitor cells, BioMed. Eng. OnLine 9 (2010) 70.